Available online at www.sciencedirect.com
SCIENCE DIRECT®
Microelectronic Engineering 81 (2005) 524–529
MICROELECTRONIC ENGINEERING
www.elsevier.com/locate/mee

Atomic and electronic structures of amorphous ZrO_2 and HfO_2 films

Vladimir Gritsenko [a], Daryja Gritsenko [a], Sergei Shaimeev [a], Vladimir Aliev [a], Kamil Nasyrov [a], Simon Erenburg [b], Vladimir Tapilin [c], Hei Wong [d,*], M.C. Poon [e], J.H. Lee [f], J.-W. Lee [f], C.W. Kim [f]

[a] *Institute of Semiconductor Physics, 630090 Novosibirsk, Russia*
[b] *Institute of Inorganic Chemistry, 630090 Novosibirsk, Russia*
[c] *Institute of Catalysis, 630090 Novosibirsk, Russia*
[d] *Department of Electronic Engineering, City University of Hong Kong, Tat Chee Avenue, Kowloon, Hong Kong*
[e] *Department of Electronic Engineering, Hong Kong University of Science and Technology, Clear Water Bay, Kowloon, Hong Kong*
[f] *Samsung Advanced Institute of Technology, P.O. Box 111, Suwon 440-600, Korea*

Available online 7 April 2005

Abstract

Atomic and electronic structures of ZrO_2 and HfO_2 films deposited using sputtering technique were studied by X-ray diffraction (XRD), EXAFS spectroscopy, photoemission (with X-ray and ultraviolet excitation sources) and electron energy loss spectroscopy (EELS). XRD results indicated that the as-deposited films were amorphous and a monoclinic phase was detected after annealing them in ambient at 800 °C. Photoemission results indicated that the ZrO_2 valence band consists of two bands separated by an ionic gap of 6 eV. The lower band of 10 eV width is occupied mainly by O 2s states. EELS results indicated that the bandgap of ZrO_2 and HfO_2 films are 4.7 and 5.7 eV, respectively.

Keywords: High-*k* dielectric; Atomic structure; Electronic structure; Charge transport

1. Introduction

The continuous shrinking of dimensions of complementary metal-oxide-silicon (CMOS) devices has led to a need to replace the silicon dioxide by higher dielectric constant insulators. Because of high dielectric constant and potential for forming device grade interfaces with Si substrate, hafnium oxide (HfO_2) and zirconium oxide (ZrO_2), with similar chemistries, have emerged as promising replacements for SiO_2 [1,2]. However, when compared with the conventional silicon oxide, high-*k* interfaces appear to have high trap density, large

* Corresponding author. Fax: +852 2788 7791.
E-mail address: heiwong@ieee.org (H. Wong).

0167-9317/$ - see front matter © 2005 Published by Elsevier B.V.
doi:10.1016/j.mee.2005.03.056

leakage current and low surface mobility [1,3]. Since carrier transport properties such as carrier injection, trapping, trap ionization or charge transport in the dielectric bulk are governed by atomic and electronic structure of the material, it is crucial to understand these important features. In this work, we explore various atomic and electronic structures of sputtered and annealed ZrO_2 and HfO_2 films by using several analytical tools.

2. Experimental

The zirconium and hafnium oxide was deposited on ⟨1 0 0⟩ *n*-type Si substrate with resistivity of 20 Ω cm using an ARC-12M sputtering machine. Before the sputtering, a standard RCA cleaning process was conducted to clean the sample. Zirconium and hafnium metal of 99% purity were used as targets for sputtering. The argon and oxygen gases were introduced into the chamber after it was pumped to 10^{-6} torr. The argon-to-oxygen flow ratio was fixed at 2:23 and the pressure of the chamber was kept at 10^{-3} torr during the sputtering. The X-ray diffraction (XRD) measurements were performed with a high-resolution powder diffractometer available in Budker Institute of Nuclear Physics in Novosibirsk. Zirconium *K* edge (Zr *K*) EXAFS spectra were measured using the synchrotron radiation (SR) of the VEPP-3 storage ring at the same Institute. The photoemission studies were performed with a VG ESCALAB 220i-XL photoelectron spectroscopy system with a monochromatic aluminum Kα source (1486.6 eV). An unfiltered He I (21.2 eV) gas-discharge lamp was used for ultraviolet photoelectron spectroscopy (UPS) study. Electron energy loss spectra (EELS) were measured using LAS-3000 Auger Electron Spectrometer.

3. Results and discussion

Fig. 1 shows the XRD spectra of both an as-deposited HfO_2 film and a sample subjected to 800 °C annealing in atmosphere. The as-deposited film shows an amorphous structure, whereas the thermal annealing results in the appearance of

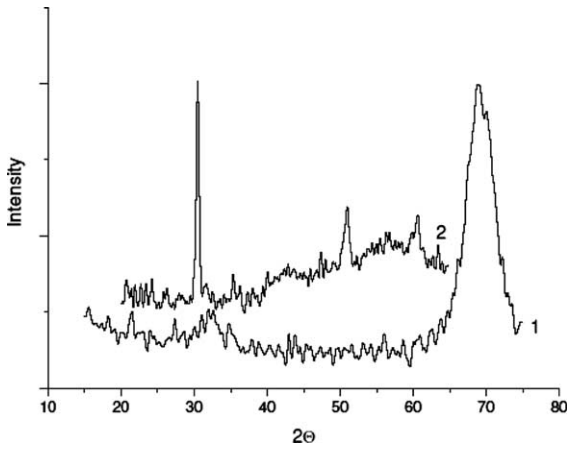

Fig. 1. X-ray diffraction (XRD) spectra of HfO_2 films: (1) as deposited, (2) annealed at 800 °C for 30 min.

the tetragonal phase. EXAFS measurement was used to study the structure peculiarities. Fig. 2 shows the radial distribution function of HfO_2. Both virgin and annealed films show pronounced peaks in the first coordination sphere corresponding to the Hf–O bond. The peak intensity increases after the thermal annealing (see trace 2). No pronounced Hf–Hf peak is found in virgin sample but in annealed HfO_2, the Hf–Hf peak is enhanced significantly. These results indicate that the as-deposited film is amorphous and it changes to

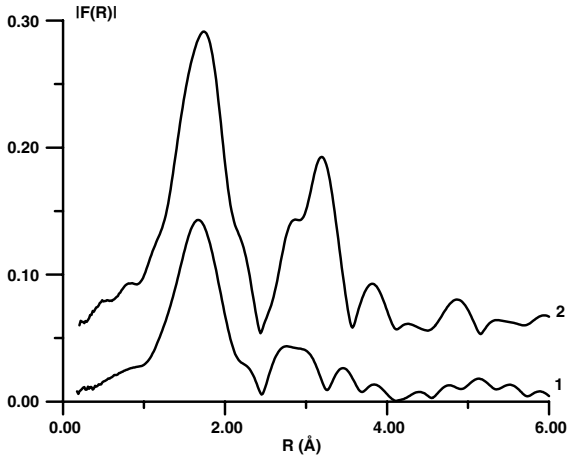

Fig. 2. Radial distribution function (normalized Zr *K* X-ray absorption coefficient) of as-deposited ZrO_2 film (trace 1) and of the sample annealed thermally at 800 °C (trace 2).

monoclinic phase after the 800 °C annealing. Fig. 3 shows the EXAFS of as sputtered and annealed ZrO_2 films. Similar phenomena are observed. The thermal annealing results in the increase of Zr–O peak intensity so that the Zr–Zr peak in the annealed sample becomes comparable to the Zr–O peak.

Band-structure program BAND which is based on Amsterdam Density Functional (ADF) was used to calculate the electronic structure of cubic ZrO_2. The spin restricted option of the program was used and no relativistic effects were taken into account. The exchange-correlation potential was described by the local density approximation (LDA). Combination of numerical atomic orbitals (NOs) from Hermann–Skillman type free atom calculation and Slater type atomic orbitals (STO) Zr 4p, 4d, 5s and O 2s, 2p, 53 functions per unit cell were treated as the valence states. Atomic NOs of core states were considered frozen. Other details of the ADF simulation can be found in the work by Velde and Baerends [4].

The lower valence band of ZrO_2 is mainly made up with oxygen 2p states and only in the lower energy part of the top band the Zr 4d states give remarkable contribution. The top of upper valence band located at X point of Brillouin zone. The lowest conduction band consists mainly the Zr 4d states. The bottom of the band is located at Γ point of the Brillouin zone. From the dispersion law, nearby Γ point along ΓX-, ΓL-, and ΓK-directions, the electron effective masses were obtained. In Γ, point there are two generated states which are split along ΓX- and ΓK-directions, and remain generated along ΓL-direction. Corresponding to these directions, we have five different electron masses with m_e^*/m_0 value in the range of 0.73–2.26. The hole masses at X point are in the range of 0.33–3.33; namely, both light and heavy holes existed.

The valence band electronic structure of the amorphous ZrO_2 and HfO_2 were studied using XPS and UPS. According to the experimental data and the quantum-chemical simulation, the ZrO_2 valance band consists of two bands: the upper band mainly consists of O 2p states with mixture of Zr 4d, Zr 5s states, and the lower band with O 2s states (see Fig. 4). Similar ZrO_2 valence band electronic structure was reported by Foster et al. [5,6]. The ionization cross-section of electron in the valence band depends on their wave function symmetry and the excitation energy [7]. At the excitation energy of 1486.6 eV, the main contribution to the electron ionization cross-section in the top valence band is due to Zr 4p and Zr 4d

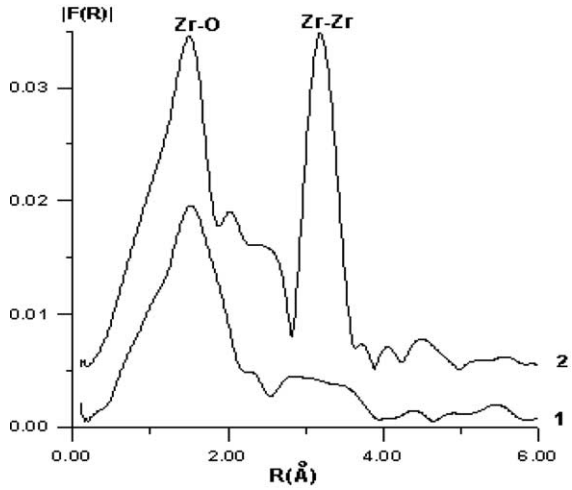

Fig. 3. Radial distribution function (normalized Hf K X-ray absorption coefficient) of as-deposited HfO_2 film (trace 1) and of the sample annealed thermally at 800 °C (trace 2).

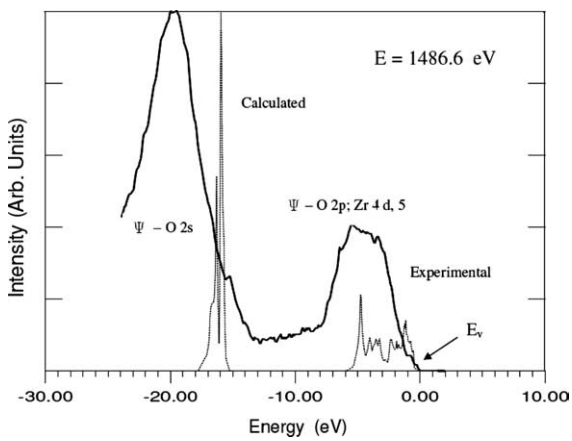

Fig. 4. Experimental X-ray photoelectron spectra (solid line) of amorphous ZrO_2 valence band (solid line) and calculated XPS valance band spectra of cubic zirconia (dashed line).

electrons. For excitation energy of 40.8 eV, the largest contributions to the electron ionization are from O 2p and Zr 4p electrons; and at excitation energy of 21.2 eV, the ionization cross-section is contributed mainly from O 2p and Zr 4d electrons.

Ultraviolet photoelectron spectrum of ZrO_2 measured at energy 21.2 eV is shown in Fig. 5 together with a gold spectrum for calibration. The low-energy threshold of UPS spectra is due to the high-energy photoelectrons. The low energy tail of UPS spectra contains information of the top position of ZrO_2 valence band. Since the work function of gold is 5.1 eV and the top of ZrO_2 valence band is 2.5 eV above the gold Fermi level, it follows that the position of the amorphous ZrO_2 valence band relative to the vacuum level is 7.6 eV. The gold Fermi level is same as the top of silicon valence band, the valence band offset (hole barrier) at Si/ZrO_2 interface is thus 2.5 eV. This value agrees with the hole barrier determined using internal photoemission and photoconductivity experiments for atomic layer deposited (ALD) ZrO_2 [8,9].

The energy gap of HfO_2 and ZrO_2 were investigated with electron energy loss spectroscopy (EELS) measurement at electron beam energy of 200 eV and the results are shown in Fig. 6. In these diagrams, the zero energy corresponds to the elastic electron peak and negative energies correspond to the inelastic energy losses. For amorphous ZrO_2 prepared using sputtering method, the measured bandgap is 4.7 eV (see Fig. 6(a)) which is in the

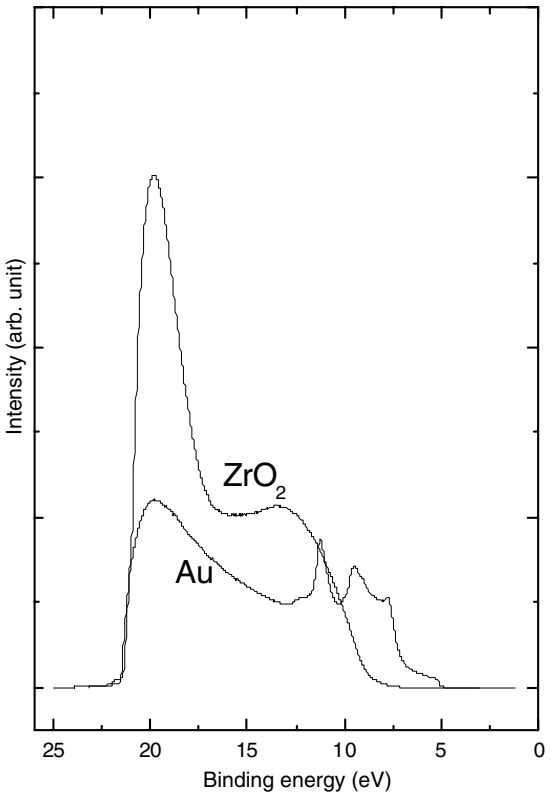

Fig. 5. Ultraviolet photoelectron spectroscopy of amorphous ZrO_2 and gold valence band excited by He I line (21.2 eV).

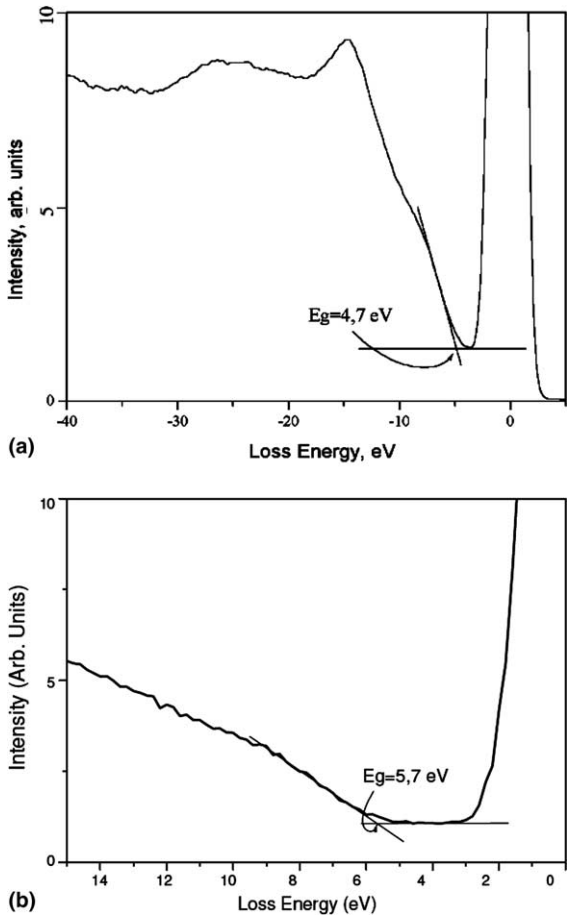

Fig. 6. Electron energy loss spectra of: (a) amorphous ZrO_2 and (b) amorphous HfO_2 at electron beam energy 200 eV. Zero energy corresponds to the elastic electron peak and negative energies correspond to the inelastic energy losses.

mostly reported range [9–11] and differs from the 5.8 eV value given by Robertson [12]. For hafnium oxide, the measured bandgap is 5.7 eV (see Fig. 6(b)). This value is in the range reported by a recent study using photoelectron emission measurements [13] and slightly less than the 6.0 eV value reported earlier [12]. Yet the differences may be due to the oversimplified procedure for extracting the bandgap data. A better approach by subtracting the zero-loss peak and restoring the loss function to determine the onset of band-to-band excitations [14] is under investigation.

Current–voltage characteristics of the p-Si/ZrO_2/Al structure measured in dark and at illumination are shown in Fig. 7. At positive biasing, current saturation due to minority carrier (electron) injection from silicon into dielectric is observed. This result indicates that the current conduction is mainly contributed by electron for positive biasing on Al electrode. In the n-Si/ZrO_2/Al structure (see Fig. 8), the current saturation occurs at negative biasing on the Al electrode and suggests that the current conduction is contributed by hole current. Hence, the current conduction in ZrO_2 is two bands resembling to the silicon nitride case.

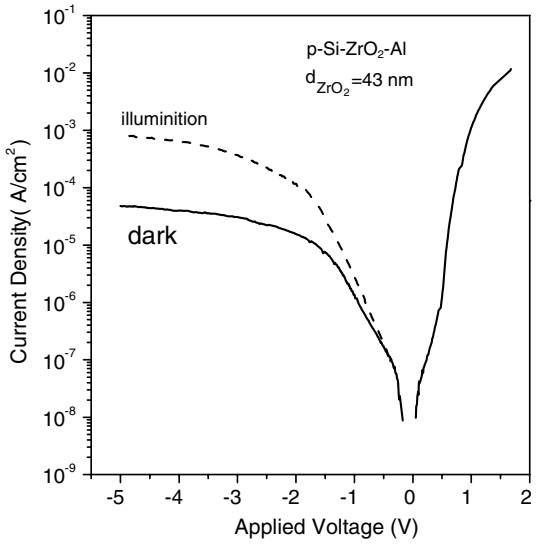

Fig. 7. Current–voltage characteristics of p-Si/ZrO_2/Al structure at both polarities in dark (solid line) and under illumination (dashed curve). The current saturation at positive Al biasing indicates the electron injection from Si into the ZrO_2 film.

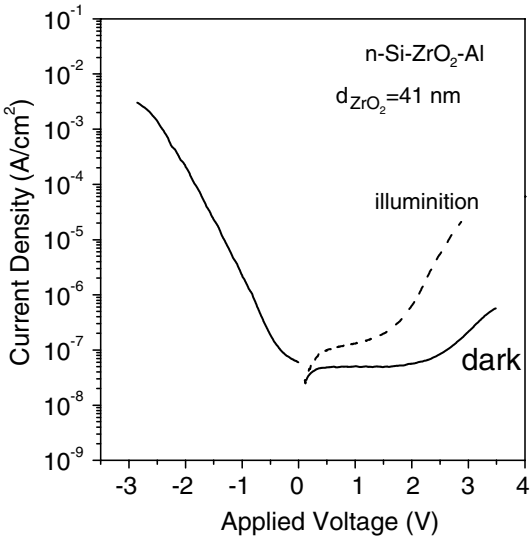

Fig. 8. Current–voltage characteristics of n-Si/ZrO_2/Al structure at both polarities in dark in under illumination. The current saturation at negative Al biasing indicates the hole injection from Si into ZrO_2.

4. Conclusion

In summary, the atomic and electronic structures of sputtered ZrO_2 and HfO_2 were investigated. Thermal annealing at 800 °C results in transferring the amorphous phase to tetragonal ones and narrow Zr–O and Hf–O EXAFS peaks were observed. Photoemission measurements indicated that the ZrO_2 and HfO_2 valence band consists of two bands separated by an ionic gap of 6 eV. The bandgaps of ZrO_2 and HfO_2 estimated from EELS are 4.7 and 5.7 eV, respectively.

Acknowledgements

This work was supported by project No. 116 of Siberian Branch of Russian Academy of Sciences, UGC Competitive Earmarked Research Grant of Hong Kong (Project No. 9040807 CityU1167/03E), and the National Program for Tera-Level

Nanodevice of the Korea Ministry of Science and Technology as one of the 21st Century Frontier Programs.

References

[1] G.D. Wilk, R.M. Wallase, J.M. Anthony, J. Appl. Phys. 89 (2001) 5243.
[2] K. Kukli, M. Ritala, J. Aarik, T. Uustare, M. Leskela, J. Appl. Phys. 92 (2002) 1833.
[3] H. Wong, K.L. Ng, N. Zhan, M.C. Poon, C.W. Kok, J. Vac. Sci. Technol. B 22 (2004) 1094.
[4] G. te Velde, E.J. Baerends, Phys. Rev. B 44 (1991) 7888.
[5] A.S. Foster, V.B. Sulimov, F. Lopez Gejo, A.L. Shluger, R.M. Nieminen, Phys. Rev. B 64 (2001) 224108.
[6] A.S. Foster, V.B. Sulimov, F.L. Gejo, A.L. Shluger, R.M. Nieminen, J. Non-Cryst. Solids 303 (2002) 101.
[7] J.-J. Yen, Atomic Calculation of Photoionization Cross-sections and Asymmetry Parameters, Gordon and Breach Science, USA, 1993.
[8] V.V. Afanas'ev, M. Houssa, A. Stesman, M.M. Heins, Appl. Phys. Lett. 78 (2001) 3073.
[9] V.V. Afanas'ev, M. Houssa, A. Stesman, M.M. Heins, J. Appl. Phys. 91 (2002) 3079.
[10] S. Miyazaki, M. Narasaki, M. Ogasawara, M. Hirose, Solid-State Electron. 46 (2002) 1679.
[11] N. Ikarashi, K. Manabe, Appl. Phys. Lett. 80 (2002) 4127.
[12] J. Robertson, J. Vac. Sci. Technol. B 18 (2000) 1785.
[13] V.V. Afanas'ev, A. Stesmans, W. Tsai, Appl. Phys. Lett. 82 (2003) 245.
[14] R.H. French, H. Mullejans, D.J. Jones, J. Am. Ceram. Soc. 81 (1998) 2549.